SLAC-PUB-12406
March 2007

# Design and Initial Tests of the Tracker-Converter of the Gamma-ray Large Area Space Telescope

W.B. Atwood,[a] R. Bagagli,[b] L. Baldini,[b] R. Bellazzini,[b] G. Barbiellini,[c] F. Belli,[d] T. Borden,[e] A. Brez,[b] M. Brigida,[f] G.A. Caliandro,[f] C. Cecchi,[g] J. Cohen-Tanugi,[e] A. De Angelis,[c,h] P. Drell,[e] C. Favuzzi,[f] Y. Fukazawa,[i] P. Fusco,[f] F. Gargano,[f] S. Germani,[g] R. Giannitrapani,[c,h] N. Giglietto,[f] F. Giordano,[f] T. Himel,[e] M. Hirayama,[j] R.P. Johnson,[a,*] H. Katagiri,[i] J. Kataoka,[k] N. Kawai,[k] W. Kroeger,[e] M. Kuss,[b] L. Latronico,[b] F. Longo,[c] F. Loparco,[f] P. Lubrano,[g] M.M. Massai,[b] M.N. Mazziotta,[f] M. Minuti,[b] T. Mizuno,[i] A. Morselli,[d] D. Nelson,[e] M. Nordby,[e] T. Ohsugi,[i] N. Omodei,[b] M. Ozaki,[ℓ] M. Pepe,[g] S. Rainò,[f] R. Rando,[m] M. Razzano,[b] D. Rich,[e] H.F.-W. Sadrozinski,[a] G. Scolieri,[g] C. Sgrò,[b,n] G. Spandre,[b] P. Spinelli,[f] M. Sugizaki,[e] H. Tajima,[e] H. Takahashi,[i] T. Takahashi,[ℓ] S. Yoshida,[i] C. Young,[e] M. Ziegler[a]

[a] *Santa Cruz Institute for Particle Physics, University of California, 1156 High Street, Santa Cruz, CA 95064*
[b] *Istituto Nazionale di Fisica Nucleare and Dipartimento di Fisica, Università di Pisa, Largo B. Pontecorvo 3, 56127 Pisa, Italy*
[c] *Istituto Nazionale di Fisica Nucleare Sezione di Trieste, Padriciano 99, 34012 Trieste, Italy*
[d] *Istituto Nazionale di Fisica Nucleare Sezione di Roma Tor Vergata, Via della Ricerca Scientifica 1, 00133 Roma, Italy*
[e] *Stanford Linear Accelerator Center (SLAC), Menlo Park, CA 94025*
[f] *Istituto Nazionale di Fisica Nucleare and Dipartimento di Fisica, Università di Bari, Via E. Orabona 4, 70126 Bari, Italy*
[g] *Istituto Nazionale di Fisica Nucleare and Dipartimento di Fisica, Università di Perugia, Via A. Pascoli, 06123 Perugia, Italy*
[h] *Università di Udine, Via Palladio, 8 Palzzo Floria, 33100 Udine, Italy*
[i] *Hiroshima University, 1-3-1 Kagamiyama, Higashi-Hiroshima, 739-8526, Japan*
[j] *CRESST and Astroparticle Physics Laboratory NASA/GSFC, Greenbelt, MD 20771, and Department of Physics, University of Maryland, Baltimore County, 1000 Hilltop Circle, Baltimore, MD 21250*
[k] *Tokyo Institute of Technology, 2-12-1 Ohokayama Meguro, Tokyo 152-8551*
[ℓ] *JAXA/ISAS, Sagamihara, Kanagawa 229-8510, Japan*
[m] *Istituto Nazionale di Fisica Nucleare and Dipartimento di Fisica, Università di Padova, I-35131 Padova, Italy*
[n] *Scuola Normale Superiore di Pisa, Piazza dei Cavalieri 7, 56126 Pisa, Italy*

*Submitted to Astroparticle Physics*

Work supported in part by US Department of Energy contract DE-AC02-76SF00515

**Abstract**

The Tracker subsystem of the Large Area Telescope (LAT) science instrument of the Gamma-ray Large Area Space Telescope (GLAST) mission has been completed and tested. It is the central detector subsystem of the LAT and serves both to convert an incident gamma-ray into an electron-positron pair and to track the pair in order to measure the gamma-ray direction. It also provides the principal trigger for the LAT. The Tracker uses silicon strip detectors, read out by custom electronics, to detect charged particles. The detectors and electronics are packaged, along with tungsten converter foils, in 16 modular, high-precision carbon-composite structures. It is the largest silicon-strip detector system ever built for launch into space, and its aggressive design emphasizes very low power consumption, passive cooling, low noise, high efficiency, minimal dead area, and a structure that is highly transparent to charged particles. The test program has demonstrated that the system meets or surpasses all of its performance specifications as well as environmental requirements. It is now installed in the completed LAT, which is being prepared for launch in early 2008.

*Key words:* gamma-ray, telescope, tracking
*PACS:* 95.55.KA

* Corresponding author and Tracker Subsystem manager.

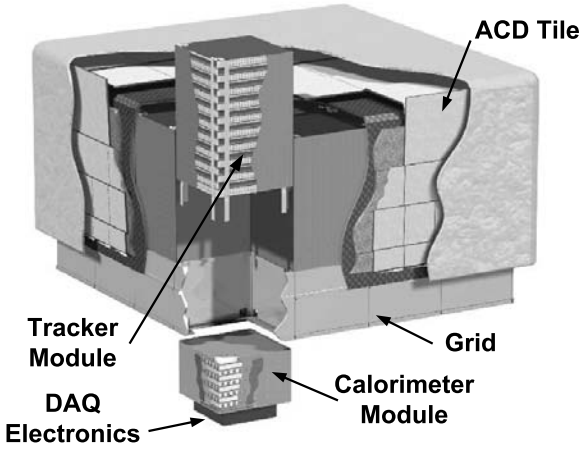


Fig. 1. Cutaway view of the LAT instrument. Each tower in the $4 \times 4$ array includes a Tracker module and a Calorimeter module.

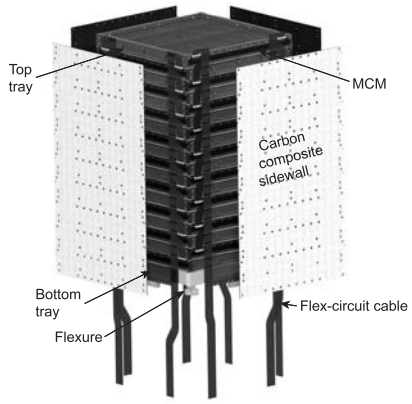


Fig. 2. Exploded view of a Tracker tower module. The detailed cable terminations at the top (Fig. 12) have been omitted from this drawing.

## 1. Introduction

The Large Area Telescope (LAT) of the Gamma-ray Large-Area Space Telescope (GLAST) mission [1][2] is a pair-conversion gamma-ray detector similar in concept to the previous NASA high-energy gamma-ray mission EGRET on the Compton Gamma-Ray Observatory [3]. High energy ($> 20$ MeV) gamma rays convert into electron-positron pairs in one of 16 planes of tungsten foils. The charged particles then pass through up to 36 planes of position-sensitive detectors interleaved with tungsten foils in the "Tracker," leaving behind tracks pointing back toward the origin of the gamma ray. After passing through the last tracking layer they enter the Calorimeter, composed of bars of cesium-iodide crystals, in a hodoscopic array, read out by PIN diodes. The Calorimeter furnishes the energy measurement of the incident gamma ray. A third detector system, the anticoincidence detector (ACD) [4], surrounds the top and sides of the tracking instrument. It consists of panels of plastic scintillator read out by wave-shifting fibers and photo-multiplier tubes and is used to reject charged cosmic-ray events such as electrons, protons or heavier nuclei.

In the LAT the Tracker and Calorimeter are segmented into 16 "towers," as illustrated in Fig. 1, which are covered by the ACD and a thermal-blanket micro-meteoroid shield. An aluminum "Grid" supports the detector modules and the data-acquisition system and computers, which are located below the Calorimeter modules.

The LAT is designed to improve upon EGRET's sensitivity to astrophysical gamma-ray sources by a factor of 30 to 100. That is accomplished partly by sheer size, but also by use of state-of-the-art particle detection technology, such as the silicon-strip detectors [5] (SSDs) used in the Tracker system.

Each of the 16 Tracker tower modules is composed of a stack of 19 "trays" supported by four sidewalls, as illustrated in Fig. 2. The trays support the active detector elements, their associated readout electronics, and the tungsten converter foils. Eight flat flexible-circuit cables connect the readout electronics to the data acquisition system located below the calorimeter, while titanium flexures and copper heat straps interface the module to the Grid.

Each tower module is 37.3 cm wide and 66 cm tall. The width, and hence the number of Tracker modules spanning the LAT, was set by the longest silicon strips that were practical to read out with good noise performance, high efficiency, and low power, while the height was optimized to give adequate lever arm between successive measurements on a track while keeping the LAT aspect ratio low to maximize the field of view. The tray structure arranges the 576 SSDs per tower into 18 $x, y$ measurement layers. Each of the top 16 layers is preceded by a plane of tungsten foils, for a total of 9 kg of tungsten, which converts about 63% of gamma rays at normal incidence into $e^+e^-$ pairs (above $\approx 1$ GeV, where the pair-conversion cross section saturates). Each $x$ or $y$ plane of silicon has 1536 strips, for a total of 55,296 readout channels per tower. The fine (0.228 mm) pitch of the strips gives excellent angular resolution for high-energy photons and provides detailed track-

ing information, which is important for reconstructing gamma-ray vertices while rejecting cosmic-ray background.

The Tracker as a whole has over 880,000 readout channels, nearly 74 $m^2$ of silicon, a sensitive area of close to 2 $m^2$, operates on only 160 W of power, and is capable of triggering at rates up to at least 10 kHz with negligible dead time. We show in the following sections how this very large quantity of state-of-the-art detectors and electronics was packaged to minimize dead area and maximize the angular resolution over a field of view greater than 2 sr, while protecting it from launch loads and other environmental factors.

## 2. Tracker System Design

The Tracker was designed to satisfy the GLAST science requirements [6] on effective area, angular resolution, and field-of-view, while fitting within the constraints of a Delta-II rocket payload fairing and respecting overall cost constraints on the mission. In addition, it was designed to provide the primary trigger of the LAT instrument. A particular challenge was to optimize the angular resolution on incoming photons over a broad range of photon energies from 20 MeV to above 300 GeV with a limited number of detector layers. The ultimate design relied on extensive Monte Carlo simulation to evaluate trade-offs between the number and spacing of the silicon layers, the SSD strip pitch, and the tungsten converter thickness. In general, the design requires a compromise between very thin converter foils, good for angular resolution, versus thick foils, good for effective area.

At low photon energy, around 100 MeV, most of the information on the photon direction comes from the first two space points measured on the track of the higher energy particle, so it is crucial that those two measurements be made close to the photon-conversion vertex, to minimize the effects of multiple scattering in the following layers of tungsten and support material. Therefore, the efficiency of each detection layer should be nearly 100%, and the inevitable inefficiencies should be localized in known regions that can be isolated at the analysis stage. Furthermore, the support material should be as transparent to photons and electrons as possible.

To avoid effects from multiple scattering in the tungsten foil in which the conversion takes place, there must be a detector layer with both $x$ and $y$ views immediately below the foil, as illustrated in Fig. 3. Thin SSDs are ideal for this purpose. They also readily achieve the desired high detection efficiency, and they operate reliably without any consumables besides electrical power.

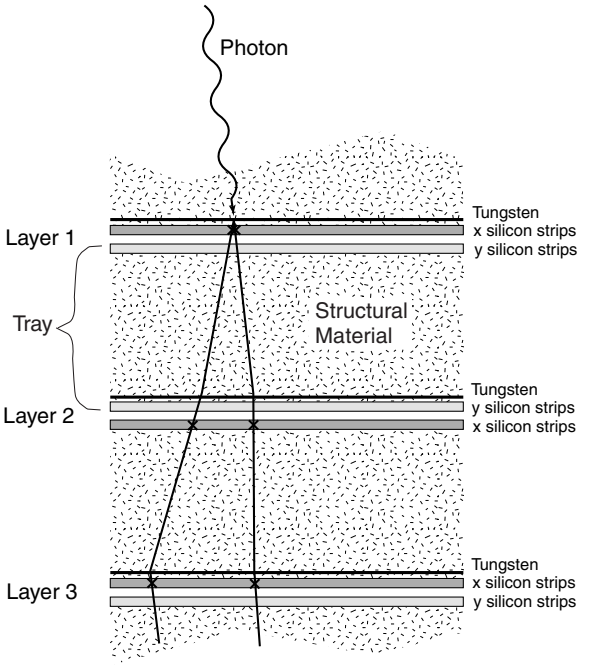


Fig. 3. Schematic depiction of the measurement of a gamma-ray conversion. Multiple scattering in successive layers degrades the angular resolution. Except at high energy, most of the angular information comes from the first two points on a track. As long as the detector layers are thin and kept very close to the tungsten foils, the measurement is impacted only by scattering in the first plane of tungsten, where the photon converts.

At very high photon energies multiple scattering is unimportant and the angular resolution is limited by the ratio of strip pitch to silicon-layer spacing. Since the layer spacing cannot be made too large without adversely narrowing the instrument field of view and raising the instrument center of gravity, the high-energy response dictates the choice of strip pitch. Furthermore, it is desirable to increase the tungsten thickness to improve the effective area for the relatively rare high-energy photons. Thicker tungsten also increases statistics at lower energies, which for many analyses involving timing studies or transients can be more important than angular resolution. Therefore, to give good performance at both ends of the energy range, the Tracker was designed

with both thin and thick converter layers. The first twelve planes of tungsten are each 2.7% radiation length (0.095 mm) in thickness, while the final four are each 18% radiation length (0.72 mm) in thickness

The Tracker mechanical structure must support and protect the detectors, electronics, and converter foils during launch, maintaining the precise locations of the detectors while using a minimal amount of material. It must also provide passive cooling paths for the waste heat of the electronics, survive worst-case temperature extremes, and serve as a shield from electromagnetic interference.

All of these considerations led to the final design with 16 Tracker modules, each assembled from 19 individual trays supporting a total of 36 planes of silicon detectors. Each tray is a stiff, lightweight carbon-composite panel with SSDs bonded on both sides, with the strips on top parallel to those on the bottom. Also bonded to the bottom surface of all but the three lowest trays of the tower, between the panel and the detectors, are the arrays of tungsten foils, one foil to match the active area of each detector wafer. Each tray is rotated 90° with respect to the one above or below. The detectors on the bottom of a tray combine with those on the top of the tray below to form an orthogonal $x, y$ pair with a 2 mm gap between them, and with the tungsten converter foils located just above. This arrangement positions both the $x$ and $y$ silicon planes closely following the converter foils while maximizing the thickness, and thus the ratio of stiffness to mass, of the supporting composite panel.

There are five variations of the tray design, which are represented in each tower module as follows: the bottom tray, which includes the interface to the Grid and has no converter foils, two mid trays with no converter foils, four mid trays with thick converter foils, eleven mid trays with thin converter foils, and the top tray, which has thin converter foils.

The gaps and amount of material between the 16 Tracker modules must be minimized to achieve optimal performance of the detector system. Mounting the front-end electronics on the sides of the tray panels greatly reduces the gaps between modules, at the expense of necessitating a right-angle interconnect between SSDs and the readout electronics multi-chip module (MCM). Thin flexible-circuit cables connect the nine MCMs on each side of a Tracker module to the data acquisition electronics, minimizing the wiring mass between modules. The use of carbon-composites for the sidewalls provides stiff support for the Tracker module with minimal scattering of particles passing from one module to another.

## 3. Detector Design

Much of the improvement in performance of the LAT over its predecessor, EGRET, arises from the use of modern silicon strip technology to track the electron positron pair produced in the photon conversion. This technology was originally developed for use in particle-physics spectrometers, where the tracking performance generally demands a minimal amount of material. In the LAT Tracker that consideration is not as important, due to the large amount of tungsten in the tracking volume, so the silicon was made about 30% thicker than is typical in particle physics, to optimize the signal-to-noise for the long strips needed in the LAT, and two layers of single-sided SSDs were used for each $x, y$ layer instead of using more expensive, complex, noisier, and less reliable double-sided SSDs. Similarly, the relatively large multiple scattering in the LAT allows the strip pitch to be made 4 to 8 times larger than typical in particle physics, keeping down the channel count and power consumption.

In general the SSD design was optimized for high reliability and for simplicity in the electronics design and the mechanical integration. Each SSD is a $8.95 \times 8.95\,\mathrm{cm}^2$, 400 $\mu$m thick single-sided detector, produced on $n$-intrinsic 15-cm wafers by Hamamatsu Photonics. The inactive region around the SSD perimeter is about 1 mm wide. The strip pitch is 228 $\mu$m, for a total of 384 strips, each of which is AC-coupled between the 56 $\mu$m wide aluminum readout strip and the $p^+$ implant. Each implant is biased by a $\approx 50$ M$\Omega$ polysilicon resistor connected to a bias ring, and the bias voltage (nominally 100 V) is connected between the bias ring and the solid aluminum electrode on the back side. Each strip has two $100\times200$ $\mu\mathrm{m}^2$ wire-bonding pads at each end, to give plenty of space for testing with probes as well as making a second bond in case the first fails.

The SSDs were required to be diced from the wafers to a tolerance of better than 20 $\mu$m, to allow the detector-plane assembly to be done by simple mechanical jigs, rather than by optical references. The depletion voltage was required to be no higher than 120 V, and the leakage current at 150 V and 25°C was required to be below 500 nA for every SSD and below 200 nA averaged over a lot. The bad

channel rate was required to be below 0.2%. The depletion-voltage and bad-channel requirements ensure close to 100% efficiency at a safe operating voltage. The required level of leakage current produces negligible shot noise. However, the current is expected to increase by about a factor of 10 from radiation damage over the course of the mission. The low initial value was well within the capabilities of the manufacturer and served to assure high quality of the SSDs selected for the mission. In fact, the quality of the SSDs used for the instrument fabrication significantly surpassed all of these requirements, with a bad channel rate of less than 0.01% and an average leakage current of 110 nA.

The SSDs were edge bonded with epoxy in series of four detectors to form ladders. The ladders were assembled on a set of 24 jigs using mechanical references to align the SSDs. The system was fast (24 ladders per day production rate) and precise, with a measured alignment of the SSDs of 2 $\mu$m rms and $\pm 10$ $\mu$m maximum. The strips were wire bonded within a ladder from one SSD to another, to make strips that are effectively 35 cm long, not including the three 2 mm inactive gaps at wafer boundaries along the length. The initial design called for the wire bonds to be encapsulated with Nusil CV-2500 silicone adhesive, but thermal stresses in the heavy-converter trays and the highly asymmetric bottom trays caused delamination of some of the encapsulation during thermal-cycle tests of the first articles. Thereafter, the encapsulation was eliminated from ladders used on those trays. In general, the ladder wire-bond encapsulation was found to be unnecessary for handling and electrical isolation, while it tended to compromise the mechanical integrity of the assembly during thermal cycles.

## 4. Electronics Design

Each SSD plane in a tower is made from four silicon ladders and is read out by a Multi Chip Modulde (MCM). Each MCM supports the readout of 1536 silicon strips across the full width of a Tracker layer. The principals goals of the MCM design were to obtain a system that is low power and extremely compact, and that has a conservative operating range to allow optimization of both the tracking and trigger functions while maintaining very low noise in the LAT environment.

A single MCM consists of a single printed wiring board (PWB) upon which are mounted 24 64-

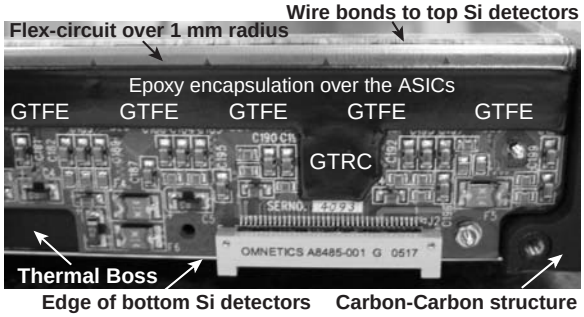


Fig. 4. Photograph of one end of an MCM mounted on the edge of a mid tray and interfaced to the SSD ladders on the tray top side. The ASICs are covered by black epoxy encapsulation.

channel front-end amplifier-discriminator ASICs (GTFE), arranged in groups of six to match the strips on four SSDs, two digital readout-controller ASICs (GTRC), the right-angle interconnect, passive electrical components, and two nano-connectors. See Fig. 4 for a photograph of one end of an MCM mounted on a tray. Each nano-connector plugs into a long multi-layer flexible-circuit cable, each of which interfaces nine MCMs to the Tower Electronics Module (TEM), a custom-design data-acquisition module located below the Calorimeter [7]. Thus on each of the four sides of a Tracker module one finds nine readout boards to support nine planes of SSDs, which send their data to the TEM via two flex-circuit cables (see Fig. 2). The two flex-circuit cables on a side are redundant, as are the two GTRC chips on each MCM. An MCM can be configured by command to read out either to the left or right or in both directions, with the split located between any pair of GTFE chips. That protects the readout from a single-point failure of a cable or of any of the ASIC chips.

The readout of hits in the tracker is binary. That is, the amplifier outputs are discriminated by a single threshold, with no other pulse-height information stored. The threshold is remotely adjustable per GTFE chip, and channels can be individually masked from the data stream, in case they are too noisy. In addition, there is an internal calibration system by which charge can be injected into any subset of channels, with an amplitude that is adjustable per GTFE chip.

The Tracker is responsible for providing the primary trigger of the LAT instrument, in addition to its tracking function. Each Tracker module has been demonstrated to trigger on and track minimum-ionizing particles in a stand-alone mode with high

efficiency. Whenever a GTFE channel goes above threshold, the MCM sends a short (adjustable up to 1.6 $\mu$s in 50 ns increments) signal to the LAT trigger processor, which generates a trigger from coincidences of multiple Tracker layers. Individual Tracker channels can be masked from the trigger (independent of the data mask), in case they are noisy. In normal operation the Tracker trigger requires a coincidence of six adjacent SSD planes in a module, formed from three $x, y$ pairs, which eliminates all but an immeasurably small contamination of random noise triggers. The asynchronous trigger signal within an MCM, formed from a logical-OR of all channels read out by a given GTRC chip, is also used by the GTRC to measure and store a time-over-threshold, which is appended to the event readout in case an instrument trigger is received. That feature provides some information on the amount of ionization, which is useful for background rejection.

The readout electronics fabrication was based on fairly standard chip-on-board technology, but the right-angle interconnect, the large number of chips, and its odd size and shape made the MCM a challenge to manufacture. The MCM ASICs were bonded directly to the polyimide-glass circuit boards and connected by more than 3000 25-micron diameter wire bonds per MCM. The wire bonds were encapsulated with epoxy, to allow the MCMs to be handled without damage during the subsequent test and assembly steps. The MCM design is described in detail in Ref. [9] and is not repeated here. Manufacturing of the MCMs is described in detail in Ref. [10], including a complete discussion of contamination problems that affected the encapsulation on early production MCMs, resulting in some delamination and loss of channels. See Section 8 for results on the number of bad channels and the particle detection efficiency.

## 5. Detector and Electronics Integration

Figure 5 illustrates the integration of detectors, converter foils, and electronics onto a carbon-composite panel to form a complete tray assembly. The SSDs are located on the top and bottom of a panel, while the readout electronics are supported on two of the panel sides. The high density right-angle interconnect, consisting of a single-layer Kapton flexible circuit and wire bonds, joins the electronics and SSDs around the 90° corner.

The tungsten converter foils are located between

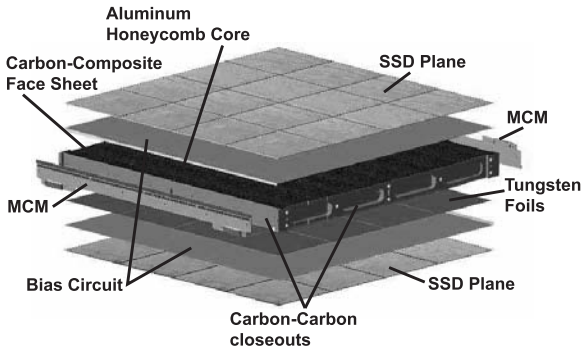


Fig. 5. Exploded view of a mid tray, illustrating the integration of detectors and electronics.

the panel and the SSDs on the tray bottom, to keep them as close as possible to the following $x$ and $y$ SSD planes. The thick foils were formed from Kulite K1750, a sintered 92.5% tungsten alloy, while the thin foils were cut from 99.95% pure rolled tungsten. The tungsten foils were etched and then primed with Cytec BR-127 to prepare their surfaces for bonding to the tray at room temperature with 3M Scotch-Weld 2216 epoxy adhesive.

Two-layer Kapton flexible circuits called "bias circuits" were then bonded to both sides of the tray with the same adhesive at a slightly elevated temperature (35°C). The top layer of the bias circuit has four gold-plated pads per SSD for making electrical contact to the SSD back sides. Those pads are routed to eight wire-bond pads on the circuit edge, where connections to the bias voltage on the MCMs are made. The bottom layer is a solid shield plane of 8.5 $\mu$m thick copper connected through 16 redundant vias to wire-bond pads, where connections are made to the 1.5 V potential on the MCM that serves as the reference for the preamplifier inputs.

The SSD ladders were bonded to the bias circuits with 19 dots of Nusil CV-1142 silicone adhesive and four dots of conductive Nusil CV-2646 silicone adhesive per SSD. The adhesive bonds, about 0.25 mm thick, remain pliable even at the lowest temperatures experienced by the Tracker and prevent excessive stress in the SSDs from thermal mismatch among the silicon, carbon-composites, and tungsten. The nominal gap between ladders, 0.2 mm, is small compared with the 1 mm inactive border of each SSD.

The alignment of the ladders to the tray was accomplished with a mechanical jig, using the reference holes on each side of the tray. This assembly technique guaranteed a planarity of 25 $\mu$m rms,

±70 $\mu$m maximum, and the measured ladder alignment is 20 $\mu$m rms, ±50 $\mu$m maximum. The alignment error is much smaller than the gap between ladders, so that no trays were lost during the ladder assembly, and is much less than the 228 $\mu$m strip pitch, so that during event reconstruction the SSDs plane can be treated as a single detector of nominal dimensions. The track reconstruction algorithm needs to consider only three alignment parameters: a shift of the SSD plane along the measured coordinate direction, a rotation of the plane around its normal direction, and a shift of the plane in the normal direction.

The 16-tower Tracker includes 576 MCMs to read out 2304 SSD ladders, for a total of 14,976 ASICs and 9216 SSDs. Each MCM reads signals from four ladders, and each tray has two MCMs to read out two SSD planes, except for the top and bottom trays, which each have a single MCM reading out a single SSD plane. The mechanical design was aggressive in minimizing dead area within the telescope aperture, and that is particularly evident in the small space in which the MCM is installed. Figure 6 shows a cross section of the edge of a mid tray, illustrating how the dead space between tower modules was kept as small as 1.79 cm (the distance from SSD to SSD, or twice the dimension called out in Fig. 6, plus the 1 mm inactive edge of each SSD). Many of the features are visible in the photograph in Fig. 4, including the MCM, a connector, the right-angle interconnect, the two detector planes, and the thermal boss, which is an integral part of the carbon-carbon closeout of the composite panel. The MCMs were bonded to the trays with 3M Scotch-Weld 2216 adhesive. Wire bonds were then made from the gold-plated traces of the right-angle-interconnect flexible circuit to the SSDs and the bias circuit.

The original design called for the wire bonds between MCMs and ladders to be encapsulated with silicone adhesive, but significant delamination occurred during thermal cycle tests of prototype trays, and the encapsulation was eliminated. That did not cause any difficulties in handling during assembly, and care was taken not to leave any conductive debris inside the tower that could eventually cause short circuits between wire bonds. In fact, no short circuits have been seen in the 1.5 years since completion of the 18 tower-module assemblies, and notably not during thermal-vacuum and vibration testing of the individual towers or the entire LAT.

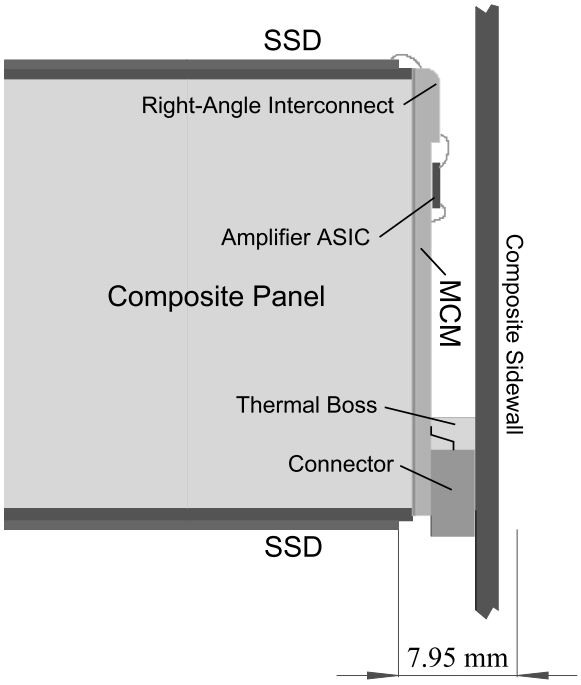


Fig. 6. Cross section of the edge of a mid tray. The dimension line gives the distance between the SSD edge and the midpoint between adjacent tower modules.

## 6. Structural and Thermal Design

The Tracker structure was designed with the following main requirements and goals in mind:

– The structure should be as transparent as possible to charged particles, to minimize multiple scattering, bremstrahlung, Compton scattering, and photon conversions in non-ideal locations. The best angular resolution is obtained when all of the gamma-ray conversions occur in the tungsten foils or in the silicon plane just below, rather than in the other SSDs or the structural material. Primarily for that reason, we built the structure as much as possible out of carbon.
– The tungsten foils should be located as close as possible to the following SSD layers, to minimize the lever arm for multiple scattering.
– The dead areas and materials between tower modules should be minimized. This requires the modules to be very stiff and well aligned, in order to maintain the small (2.5 mm) gaps between them.
– Each tower module must mount to the grid with sufficient accuracy to maintain the small gaps between them.
– The structure must provide good heat conduction paths from the electronics boards to the Grid, to

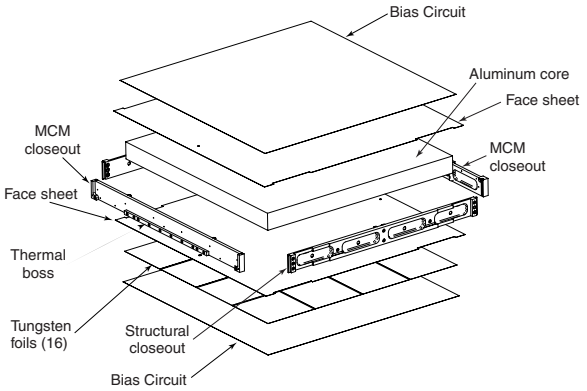


Fig. 7. Exploded view of a composite panel plus converter foils and bias circuits.

keep the differential temperature between the bottom and the hottest SSD less than 7.5°C while operating in vacuum.

– The structure must survive random vibration at NASA-specified GEVS [8] levels without damage and without contact between successive SSD planes or between adjacent Tracker modules.
– The structure must survive thermal-vacuum cycles from −15°C to 45°C without damage to the structure or, especially, to the SSDs and electronics.
– Each tower-module must vent all contained air on a timescale short compared with the launch.

The fundamental design concept is to support the SSDs and readout electronics on flat honeycomb panels, which are about 3 cm thick in the case of the mid trays. See Fig. 7 for an exploded view. Such panels can be made very light while maintaining excellent strength and stiffness. The gap between the two SSD layers in an $x, y$ pair was designed to be only about 2 mm, in order to keep both layers close to the tungsten foils bonded to the bottom of the panel. This translated into a stiffness requirement on the tray, that its fundamental drum-head mode have a frequency of at least 500 Hz, in order to be safe against collisions between trays during $z$-axis vibration.

The panel cores are vented aluminum honeycomb, with a density of 48 kg/m$^3$ for the heavy-converter and bottom trays and 16 kg/m$^3$ for the others. The face sheets are made from six plies (heavy-converter and bottom trays) or four plies (other trays) of Nippon Industries YSH50 fibers, with YLA Inc. RS-3 cyanate ester resin. The four-ply face-sheet lay-up is unbalanced and tends to curl, but the sandwich of two face sheets and core is designed to be balanced. The face sheets were bonded to the cores in an autoclave using a Redux 312UL film adhesive.

Carbon-carbon material is used for the panel closeouts because of its high thermal conductivity ($\approx$ 200 W/mK) and the ease with which it can be machined while maintaining smooth surfaces. The material was manufactured with a 3-D needled fiber preform, yielding fairly uniform mechanical and thermal properties in all dimensions, again making it suitable for machining the intricate shapes needed for supporting the MCMs as well as interfacing to the sidewalls. After carbonization, the material was backfilled with a small amount of Epon 9405 resin. Pockets were machined in the closeouts to minimize the amount of material at the tower-module edge. Threaded aluminum inserts, or titanium inserts for top and bottom trays, were bonded into the machined closeouts for the sidewall mounting screws, using a custom jig to ensure precision alignment between the closeout reference holes and all of the screw holes.

The closeout pieces were bonded to each other and to the honeycomb sandwich at room temperature using a precision steel jig and Hysol EA934NA adhesive. This procedure ensured $\pm 100$ $\mu$m precision in the lateral tray dimensions, which was crucial for the tower assembly step described below. As required for noise suppression, an electrically conductive connection between the core and and the carbon-carbon closeouts was guaranteed by compressing between the two a small (1 cm diameter) cylinder of copper-coated Kapton, bonded to core and closeout with conductive adhesive (Nusil CV2646). The tungsten foils and bias circuits were bonded to the panels, as discussed in Section 5, prior to trimming the face sheets and circuits flush with the closeouts. The cut edges and the carbon-carbon material were coated with Aeroglaze Z306 black polyurethane paint to prevent release of conductive fibers and dust.

The bottom-tray closeouts are much stronger than the others, because they form the interface of the entire tower module to the Grid. Therefore, they were made from a Toray M55J carbon-fiber woven fabric composite with a veneer of carbon-carbon bonded to it. The intricate machining was done only in the carbon-carbon veneer. The bottom-tray corners are reinforced by titanium brackets, illustrated in Fig. 8, which carry most of the load from the sidewalls into the Grid interface. Figure 10 illustrates an assembled bottom tray viewed from below, such that the single plane of SSDs on the top surface is not visible.

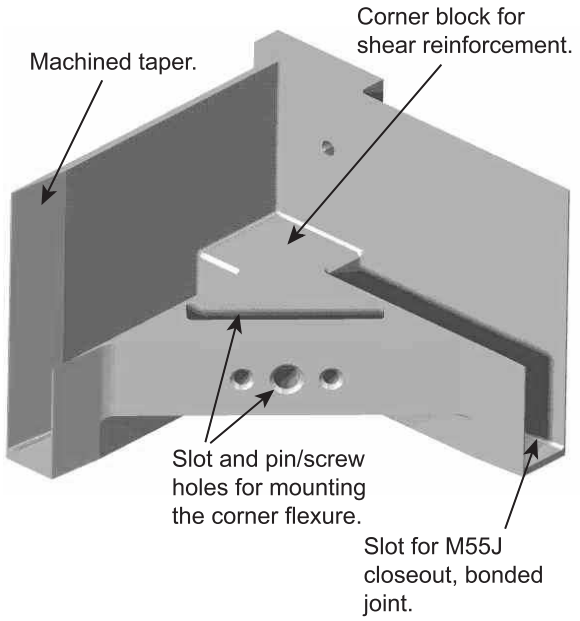


Fig. 8. Titanium corner bracket used to reinforce the bottom trays and to which the corner flexures are attached.

Flat carbon-composite sidewalls support the stack of trays in a stiff box structure. Each sidewall is composed of twelve layers of Mitsubishi K13D2U fibers with two layers of Nippon-Graphite SF-YS90A-75 fabric on each side, all bonded with CE3 cyanate-ester resin (prepreg from COI of ATK Space Systems). There is also 25 $\mu$m of aluminum foil bonded on each side for electrical shielding, and the aluminum was painted black with Aeroglaze Z-306 on most of the outer surface to increase the thermal emissivity. More than 160 screws attach each sidewall to the trays. Because the load of the entire tower passes from the walls into the bottom tray, the bottom-tray interface is much more rugged than those of the mid trays and top tray, each of which supports only a single tray. For the bottom tray only, titanium inserts were bonded into the sidewall screw holes to support the 100° countersink screw heads. For the other trays, 120° countersink holes were machined directly into the carbon-composite material.

For tower assembly, the 19 trays were stacked in their final configuration, inverted, on a steel tower assembly jig (Fig. 9). The trays were referenced to the precision reference walls of the jig with pins that couple the jig holes with the trays reference holes. After the tray positioning, the eight cables were mounted, and a TEM was installed and connected to the cables. The tower was enclosed in a dark box and fully tested by monitoring cosmic-ray


Fig. 9. A tower module being assembled inverted in the precision steel assembly jig, shown during the cable mounting step.

events. After the functional test, the sidewalls were installed on the two free sides. The two steel reference walls were then replaced one at a time by the other two sidewalls. The alignment of the trays is maintained by the countersunk screws holding the sidewalls to the trays. Monitoring of the relative positions of the SSDs planes by tracking cosmic rays demonstrated a very stable setup, with maximum relative displacements of the trays of $\pm 20$ $\mu$m after transportation and environmental tests.

M2.5 screws were used to fasten the sidewalls to the trays, except for four M4 screws per sidewall that fasten into the bottom tray. The screw heads were Torx+, as hex heads in these small sizes were found to be unable to support the needed torque. The 120° countersink screws were custom made and were found to be essential, compared with the standard 100° countersink, to prevent damage to the carbon-composite sidewalls.

The bottom tray interfaces mechanically to the Grid through eight flexures, one on each corner,

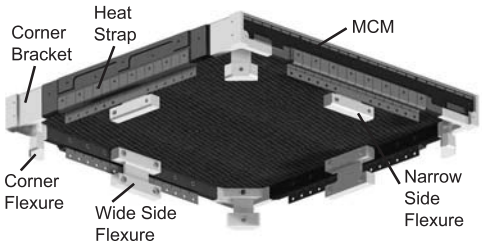


Fig. 10. Drawing of a bottom tray, showing the titanium flexures and copper heat straps that interface to the Grid. Note: this rendering of the flexures does not show their conical holes at the Grid interface.

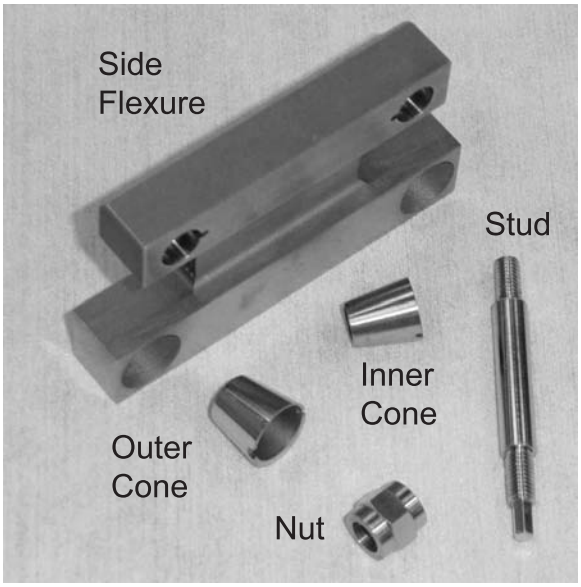


Fig. 11. Photograph of a side flexure and some of the Grid interface hardware, including the eccentric cones that allow the tower alignment to be precisely adjusted while maintaining a tight fit.

mounted in the corner bracket, and one at the center of each side, bolted into inserts in the tray, as illustrated in Fig. 10. The three-blade flexures are oriented such that the Grid can expand and contract with temperature variations without putting significant stress into the carbon-composite structure. Half of the side flexure mounts are wider than the others, so that the studs and nuts between flexure and Grid do not interfere between neighboring tower modules.

The interface to the Grid was greatly complicated by the limited precision that could be achieved for both the tower-module assembly and, to a lesser extent, the drilling of the Grid. Match drilling the tower modules and Grid was not practical, and the holes could not be drilled oversized, as the vibration requirements would not allow the Trackers to be held in position by friction. Therefore, the holes in the flexures were made conical, to ensure a tight fit, and two eccentric nested cones (one stainless steel, the other titanium) were inserted between the flexure hole and the mounting stud. [1] By rotating both of the nested cones, the hole location for the stud could be adjusted to any point within a 1 mm radius. Shims were also placed between the flexures and the Grid. By adjusting the shims and cones, we could install the Trackers in the Grid accurately aligned, with near zero-clearance joints, and without inducing significant stress into the carbon-composite structure. Figure 11 is a photograph of one flexure, the cones, a stud, and a nut.

In practice, the cones in three corner flexures were oriented by calculation, based on detailed measurements of the tower module and its flexures made by an automated coordinate measuring machine (CMM). After securing the tower module to the Grid by just those three flexures, the nine remaining pairs of cones were individually adjusted to compensate for as-built manufacturing tolerances in the Grid as well as the Tracker.

Besides supporting only a single plane of SSDs, the top tray is also special in that it supports the termination of four of the eight flex-circuit readout cables. Those four cables have arms that point downward to connect into inverted MCMs, and the upper end must extend above the top tray to provide room for routing traces and soldering termination resistors, while keeping all vias out of the bend region. As in the case of the bottom tray, the top tray core is thinner than those of mid trays and its closeout extends upward past the core. The extended closeouts provide inserts for attaching a tower-module lifting fixture and also support the cable terminations. Figure 12 shows the terminations of two flex-circuit cables, which are bent 180° over machined aluminum brackets that are bonded to the closeout. Aluminum clips secure the cable ends. The bracket also supports a removable nest for a solid alignment

[1] The "Eccentric Conical Fastening System" was invented at SLAC during the course of the LAT project. The inventor, Eric Gawehn, has since left SLAC and has filed patent applications for the invention.

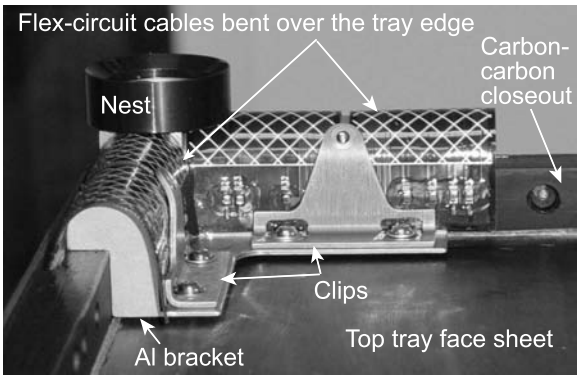


Fig. 12. Photograph of a corner of a top tray, showing the flex-circuit cable termination and an alignment-ball nest. In the finished tower module, most of what is seen here is covered by aluminum foil and then black paint.

ball, used in the tower-level CMM survey, or retroreflector ball, used in the optical survey of the Tracker mounted on the Grid.

In addition to supporting the trays, the sidewalls also serve to conduct the waste heat from the electronics down to the Grid. The bottom tray and sidewalls are thermally tied to the Grid by copper heat straps, as illustrated in Fig. 10. Each strap is composed of two layers of 0.38 mm thick copper. On the Tracker side they are bonded between the sidewall and bottom tray, while on the Grid side they are clamped dry between an aluminum bar and the Grid.

Heat from the MCM ASICs flows through the conducting adhesive that bonds them to the printed wiring board (PWB), through the PWB, aided by several copper planes and numerous copper vias, through about 0.2 mm of epoxy, and into the high thermal-conductivity carbon-carbon closeout. The closeout includes an integral thermal boss that is tightly bolted to the sidewall with eight screws. Because the MCM dissipates only 0.25 W, the power density on the MCM (area $> 83\,\mathrm{cm}^2$) and in the thermal boss (area of $0.6 \times 20\,\mathrm{cm}^2$) is so small that the temperature drop from MCM to sidewall is negligible. The sidewall composite has a measured thermal conductivity of 216 W/mK in the vertical direction (similar to typical aluminum alloys). In a thermal-balance test carried out on a mechanical prototype (with resistive heaters substituted for the electronics boards), we measured a temperature drop of only $\approx 5°\mathrm{C}$ from the top of the tower module to the bottom when it is operated at nominal power in vacuum with its radiative cooling blocked by a temperature-controlled shield. An estimated additional drop of $\approx 2°\mathrm{C}$ occurs in the interfaces between the bottom tray closeout and the Grid.

In flight there will be a significant radiative dissipation of power from the Tracker to the ACD. Because of that, and because the Grid temperature rises from the edge to the center, the four Tracker modules in the center of the array will be the hottest, and the hottest trays are expected to be four or five layers down from the top. By design, all of the Tracker SSDs will operate well under 30°C, which will be important in keeping the SSD leakage current low toward end of life, when some radiation damage will have occurred.

## 7. Environmental Testing

The tracker must withstand the rigors of launch and the environmental conditions anticipated on orbit during both normal operations and contingency situations. Our environmental test program tested the detector subassemblies at many stages of assembly, with the most stringent test conditions used for the lowest levels of assembly [11]. Many design issues were uncovered and corrected during the application of this process to the prototype and first-article assemblies, and during the production of the flight articles, faulty subassemblies were rejected before being incorporated into trays or tower modules.

Each tower module was independently vibration tested to NASA specifications on 3 axes, with sine vibration from 5 Hz to 50 Hz and random vibration from 20 Hz to 2 kHz. The sine vibration had a maximum acceleration of 4.7 g vertically and 2.6 g laterally (and about double those accelerations for the first, protoflight tower-module), while the random vibration rms acceleration was 6.1 g vertically and 6.7 g laterally. The vertical-axis random vibration spectrum was notched by $-11$ dB around the fundamental resonant frequency of about 370 Hz, while the lateral-axis vibration was notched by $-5.5$ dB around the 130 Hz fundamental. In addition, the entire LAT underwent sine-vibration testing and acoustic testing, during which the Tracker modules experienced loads lower than in the tower-module level testing. No problems were encountered during any of the vibration testing of the protoflight and flight tower modules. In particular, the bad-channel count was not affected by the vibration tests.

All tower modules were tested for conductive electromagnetic emissions and susceptibility, and one module was tested in addition for radiative emis-

sions and susceptibility [9]. All electromagnetic interference tests, conductive and radiative, were carried out on the assembled LAT. The only Tracker problem found was a radiative susceptibility around 99 MHz, at which point the Tracker exceeded the maximum allowed noise occupancy (hits in $> 0.01\%$ of the Tracker channels) by up to a factor of ten when exposed to an intense (20 V/m) vertically polarized beam. No such radio source exists on the satellite, however, so it could be at worst a momentary problem if GLAST were to pass through a powerful radar beam.

Thermal testing was carried out at several levels. The MCMs were thermal cycled and burned in as described in Ref. [10]. Fully assembled trays underwent four thermal cycles at atmospheric pressure between $-15°$C and 45°C. Then each tower module independently underwent four thermal-vacuum cycles between $-15°$C and 45°, with comprehensive performance tests carried out at the hot and cold plateaus as well as at room temperature. In addition, the assembled LAT went through four thermal-vacuum cycles during which the Tracker temperature ranged from about 5°C to 40°C. After completion of the tests, all 14,976 Tracker IC chips were still functional. Two GTFE chips gave errors when reading back mask configuration registers, but the registers did load correctly and were therefore usable. In regions affected by the encapsulation problems mentioned in Sections 3 and 4, the numbers of disconnected channels increased slightly during thermal-vacuum testing. The total bad-channel percentage after environmental testing is given in Section 8. The environmental test activities and results are described in more detail in Ref. [11].

## 8. Test Results

The completed Tracker meets all of its design requirements in terms of power consumption, noise occupancy, efficiency, passive cooling, mass, and dimensional tolerances. It has also completed all of its environmental tests, both at the tower-module level and at the level of the full LAT. The Tracker performance is summarized in Table 1 and discussed in more detail below. Figure 13 shows a typical photon conversion detected in a beam test of an assembly of two Tracker modules and three Calorimeter modules. The rms resolution of the coordinate measurement in the plane of the silicon, perpendicular to the strip direction, was verified in additional beam tests with very high energy minimum-ionizing protons at normal incidence to be consistent with the value $\sigma = 66\ \mu$m, as expected from the 228 $\mu$m strip pitch divided by $\sqrt{12}$.

Table 1
Summary of Tracker Performance Metrics.

| Metric | Measurement |
|---|---|
| Active area at normal incidence | 1.96 m$^2$ |
| $\gamma$-ray conversion probability | 63% |
| Active area fraction within a Tracker module | 95.5% |
| Overall Tracker active area fraction | 89.4% |
| Single-plane hit efficiency in active area | $> 99.4\%$ |
| Dead channel fraction | 0.2% |
| Noisy channel fraction | 0.06% |
| Noise occupancy | $< 5 \times 10^{-7}$ |
| SSD strip spacing | 0.228 mm |
| Power consumption per channel | 180 $\mu$W |
| Tower-module mass | 32.5 to 33.0 kg |
| Maximum misalignment at top of module | 0.59 mm |
| Maximum misalignment at bottom of module | 0.29 mm |

Overall, the Tracker's efficiency and noise performance are remarkably good. The efficiency for a single silicon plane to detect a minimum-ionizing particle (MIP) passing at nearly normal incidence through the active area is $> 99.4\%$ for all but one of the flight tower modules, the first one built, for which the efficiency is 98.6%, as further discussed below. The fraction of frontal area of the full 16-module tracker that is active is 89.4%, while the active fraction within a plane of four ladders is 95.5%. The noise occupancy, or the probability for a single channel to have a noise hit in a given detector trigger, is less than $5 \times 10^{-7}$ after masking noisy channels (0.06% of the channels). More details on the detector performance metrics can be found in Refs. [9] and [12].

The tower-module measured masses range from 32.5 kg to 33.0 kg, for a total Tracker mass of 524.5 kg. The measured power consumption, with the 20 MHz clock operating, is 160 W of conditioned power for the combined set of 16 tower modules, which corresponds to $180\,\mu$W per channel. There is no measurable variation in power consumption with event rate.

The passive Tracker cooling works as planned. During operations we cannot measure the SSD or MCM temperatures, but there are 2 thermistors located at various heights on each of the 128 readout

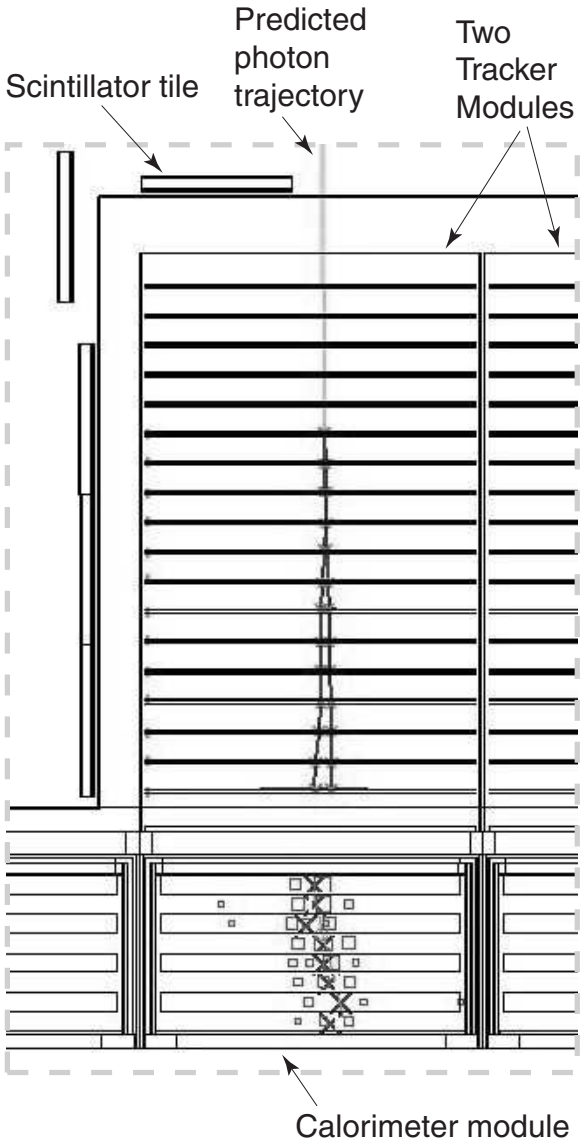


Fig. 13. Computer reconstruction of a 470-MeV photon conversion in one of two Tracker towers operated together with Calorimeter modules in a tagged-photon beam test at CERN.

flex-circuit cables. During LAT thermal-vacuum testing, the highest temperature measured in the Tracker, from thermistors located about five trays down from the tops of the four central tower modules, was 10°C above the Grid temperature at the tower-module base, which is only a few degrees higher than estimated from the thermal-balance test discussed in Section 6. The discrepancy is probably mostly in the estimate of the temperature difference across the interface between the Tracker wall and the Grid.

Following completion of the assembly of the 16

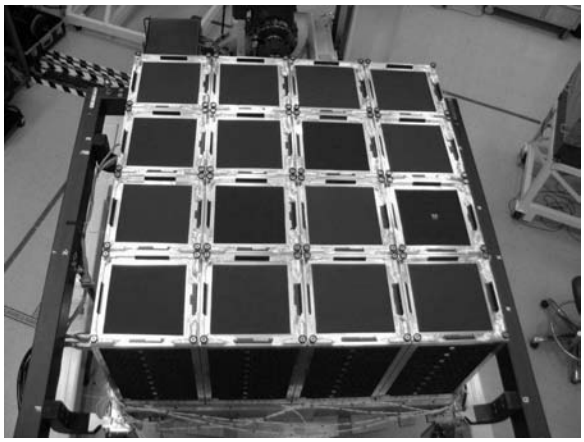

Fig. 14. Photograph of the completed Tracker, mounted on the Grid prior to installation of the ACD.

flight Tracker modules onto the Grid (Fig. 14), an optical alignment survey was conducted on the Tracker using four retro-reflector balls per tower module, mounted on nests as shown in Fig. 12. In the CMM tower-level survey, each tower module was verified to be within its stay-clear allocation. The vertical tolerance, in $z$, is large and unimportant, but the nominal tower-module width in either $x$ or $y$ is only 0.75 mm smaller than the stay-clear. The modules are generally slightly larger than nominal. Nevertheless, all of them fall within their stay-clear, with the smallest clearance equal to 0.08 mm, demonstrating a remarkably precise assembly of the composite structures.

The optical survey then verified that each stay-clear was positioned on the Grid within allowable offsets, to ensure adequate spacing between modules for dynamic and thermal motions. The top of each stay-clear was allowed to deviate horizontally by up to 0.64 mm, while the maximum excursion measured was 0.59 mm. The bottom of the stay-clear, near the Grid, was allowed to deviate horizontally by up to 0.29 mm, and there the maximum was measured to be 0.23 mm. Thus the tower modules are all adequately aligned from the mechanical viewpoint. The measured deviations are significant from the point of view of reconstructing tracks that pass from one module to another, so they will be used by the tracking software, along with further refinement based on statistical analysis of a large sample of muon or proton tracks that pass through multiple modules.

While the system satisfies the requirements and goals for detection efficiency and for low noise, a few imperfections have been noted. In particular, the first tower module fabricated suffers from an anoma-

lously high number of dead or partially-dead channels (4%) and correspondingly lower hit efficiency than found in the later modules, for which the number of dead channels is only 0.2% on average. In the original planning, that module was intended to be a qualification unit and flight spare, but schedule exigencies led to it being installed as the first flight unit. Fabrication problems encountered with it were corrected in the later modules. Those problems included the ladder wire-bond encapsulation problems mentioned in Section 3 and contamination problems that affected the wire-bond encapsulation on some MCMs, discussed in detail in Ref. [10]. Ladder wire-bond breakage generally leaves the channel functional over part of its original length. Furthermore, in the case that an isolated strip is inactive, a particle passing through that point will often be detected by the neighboring strips. For those reasons, the tower with 4% bad channels still has a single-plane efficiency of $> 98\%$ on average. However, its bad regions are non-uniformly distributed over its 36 planes of SSDs.

The only problem seen in the noise performance is that occasional bursts of coherent noise occur in 23 of the 576 SSD planes (4%), both in vacuum and at atmospheric pressure. Each burst affects a single SSD ladder, with numerous simultaneous hits in that ladder. However, there is no correlation from one SSD plane to another, so they do not impact the instrument trigger rate. They are sufficiently rare and affect so few layers that the overall average noise occupancy and data volume are not significantly impacted, and the gamma-ray conversion tracking is not adversely affected. Furthermore, we have verified that the ladder is alive and still sensitive to particles at the time of a burst. Their origin is still a mystery, as their occurrences are so random and infrequent that throughout our test program no correlation has yet been observed with bias voltage, pressure, humidity, or electromagnetic radiation. There is also no common special feature known about the fabrication or quality of the affected layers. The one correlation that has been observed is an increase in frequency of the bursts during the hot soak of thermal vacuum testing and a complete lack of bursts during the cold soak.

## 9. Conclusion

The Tracker has been fully fabricated and installed in the GLAST LAT science instrument, which has passed all of its environmental and functional tests and is being integrated with the spacecraft. The testing has verified that the Tracker satisfies and often exceeds its design requirements. It is the largest silicon-strip detector system ever built for operation in orbit, both in terms of silicon area (73.8 $m^2$) and number of readout channels (884,736) and is, in fact, surpassed in either category among terrestrial experiments by only the silicon-strip trackers being assembled for the CERN Large Hadron Collider. That such a large-scale system could be designed for operation in orbit was made possible by the development of a fully custom readout system that has a very low noise occupancy and consumes far less power per channel than any of its predecessors. The mechanical/thermal structure of the Tracker is equally innovative. It was aggressively designed to be highly transparent to charged particles, to have minimal dead area, to cool passively, and at the same time to support the detectors and electronics in precise locations while protecting them from launch loads.

The Tracker is the heart of the LAT instrument, being responsible for converting gamma rays, triggering the instrument, and measuring the direction of each photon. With its completion, the GLAST mission is now moving forward toward a launch in early 2008 and thereafter an exciting new era of gamma-ray astrophysics.

## 10. Acknowledgements

We would like to acknowledge the engineering teams at SLAC and INFN for their work on the design and fabrication of the Tracker, the LAT integration-and-test team and the electronics group at SLAC for providing the data acquisition hardware and software used to test Tracker modules, and the LAT integration-and-test team for the assembly of the completed Tracker modules into the LAT and the ensuing functional and environmental testing. We thank the NASA personnel from the Goddard Space Flight Center who worked to support the Tracker team, in particular Tom Venator, who worked closely with the team in the U.S. and Italy, and Phil Goodwin, for his help with the flex-circuit cable manufacturing. We also thank the dedicated team who set up and operated LAT detector modules in the beam tests at CERN and analyzed the data, and we thank Leon Rochester, Richard Hughes, and other LAT team members

for their careful reading of the manuscript and the helpful feedback that they provided.

This work was supported in part by the U.S. Department of Energy, under Contract DE-AC02-76SF00515 and Grant DE-FG02-04ER41286, by NASA under NAS5-00147, by the Japan-US Cooperation Program in the field of High Energy Physics, by Grant-in-Aid from the Japanese Ministry of Education, Culture, Sports, Science and Technology (14079206), and by the Agenzia Spaziale Italiana (ASI).

## References

[1] W.B. Atwood, "GLAST: applying silicon strip detector technology to the detection of gamma rays in space," Nucl. Instrum. Meth..A, vol. 342, p. 302, 1994.

[2] N. Gehrels and P. Michelson, "GLAST: the next-generation high energy gamma-ray astronomy mission," Astropart. Phys., vol 11, p. 277, 1999.

[3] D.J. Thompson, et al., "Calibration of the Energetic Gamma-Ray Experiment (EGRET) for the *Compton Gamma-ray Observatory,*" ApJ Suppl., vol. 86, pp. 629-656, June 1993.

[4] A.A. Moiseev, et al., "The Anti-Coincidence Detector for the GLAST Large Area Telescope," in press, Astroparticle Physics.

[5] T. Ohsugi, et al., "Design and properties of the GLAST flight silicon micro-strip sensors," Nucl. Instrum. Meth. A, vol. 541, p. 29, 2005.

[6] "GLAST Project Science Requirements Document," NASA GSFC 433-SRD-0001.

[7] Leonid Sapozhnikov, "Tower Electronics Module (TEM) Specification and ICD," Stanford Linear Accelerator Center GLAST/LAT internal document LAT-SS-00288, 2004.

[8] General Environmental Verification Specification for STS & ELV, NASA Goddard Space Flight Center.

[9] L. Baldini et al., "The Silicon Tracker Readout Electronics of the Gamma-Ray Large Area Space Telescope," IEEE Trans. Nucl. Sci., vol. 53, pp. 466-473, Apr. 2006.

[10] L. Baldini et al., "Fabrication of the GLAST Silicon Tracker Readout Electronics," IEEE Trans. Nucl. Sci., vol. 53, pp. 3013-20, Oct. 2006.

[11] M.N. Mazziotta et al., "Environmental Tests of the Flight GLAST LAT Tracker Towers," to be submitted to Nucl. Instrum. Meth. A.

[12] H. Tajima, "GLAST Tracker," Nucl. Instrum. Meth. A, vol. 569, pp. 140-143, 2006.